ACS Photonics

pubs.acs.org/journal/apchd5

Letter

Quantum-Memory-Enabled Ultrafast Optical Switching in Carbon Nanotubes

Kankan Cong,[‡] Weiwei Jiang,[‡] Bryan E. Anthonio, G. Timothy Noe, Huaping Liu, Hiromichi Kataura, Mackillo Kira,[*] and Junichiro Kono

Cite This: *ACS Photonics* 2020, 7, 1382−1387

Read Online

ACCESS | Metrics & More | Article Recommendations | Supporting Information

ABSTRACT: Optical nonlinearities can be engineered into high-speed optical gates when a probe signal is switched coherently and fast by an optical control pulse through various nonlinear effects for switching. In semiconductors, a strong light−matter interaction can also excite many electrons to interact with each other, which can deteriorate switching through Coulomb-induced dephasing. Here, we demonstrate that optical transmission of carbon nanotubes can be switched reversibly hundreds of times via detuned Rabi splitting, faster than 200 fs via nonresonant but strong control pulses. Our detailed experiment−theory analysis identifies that quantum memory in Coulombic scattering restores reversibility while simultaneously reducing undesirable pure dephasing of coherences. This capability creates new possibilities for ultrafast quantum optoelectronic processing in quantum materials.

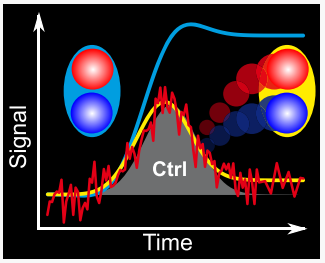

KEYWORDS: *ultrafast switching, quantum memory of many-body nonlinearities, excitonic Stark shift, quantum optoelectronics, carbon nanotubes*

High-speed optical gates[1−8] can be realized when a probe signal can be switched from on to off state nearly perfectly, coherently, and fast by an optical control pulse. While the switching itself can be created by any optical nonlinearity, its scope can be significantly expanded through strong light−matter interactions offering a broad range of nonlinear effects such as the Autler−Townes effect,[9,10] Mollow splitting,[11,12] vacuum Rabi splitting,[13−16] and ultrastrong and deep strong coupling.[17,18] In this context, semiconductor-based optical switches are both beneficial, due to direct compatibility with other semiconductor technology, and challenging because strong light−matter interaction can introduce strong light absorption that excites many electrons and holes (electronic vacancies) to interact with each other. The resulting Coulomb interaction can bind electrons and holes into excitons or can destroy coherences relevant for switching[19] through excitation-induced dephasing.[20−23] The latter often introduces irreversibility to the nonlinear system response, which prevents successive quantum operations even when light−matter interaction is made strong.

To simultaneously exploit strong light−matter interaction and eliminate irreversible many-body scattering, we propose a concept illustrated in Figure 1a. Excitations can become transient, adiabatic following when the control field $E_{\mathrm{ctrl}}(t)$ is detuned by $\Delta \equiv \hbar\omega_{\mathrm{control}} - E_{1s}$, well below the 1s-exciton absorption resonance centered at energy E_{1s}. Having strong light−matter interaction makes it possible to induce large changes to the optical response during the pulse. Since exciton binding localizes electrons with respect to holes, it enhances light−matter coupling resulting in an effective dipole d. For the highly detuned situation studied here, the exciton resonance is Stark-shifted according to a detuned Rabi splitting[19]

$$\Delta E = \frac{1}{2}\left(\sqrt{\Delta^2 + d^2 E_{\mathrm{ctrl}}(t)^2} - |\Delta|\right) \rightarrow \frac{d^2 E_{\mathrm{ctrl}}(t)^2}{4|\Delta|} \quad (1)$$

for sufficiently large detunings. Our concept relies on an ultrafast control pulse, $E_{\mathrm{ctrl}}(t)$, to nonlinearly blue-shift the 1s-exciton resonance and having particularly strong quantum-memory effects on Coulombic scattering, which unexpectedly keeps the excitation coherent and adiabatic even at high excitation levels. Only by combining these two quantum phenomena, we demonstrate that coherent dynamics prevails, making ultrafast and nearly perfectly reversible switching possible.

We use carbon nanotubes as candidates for providing the needed direct-bandgap semiconductor[24] with a large 1s-exciton binding energy[25−27] in order to provide the needed strong light−matter coupling.[28] Such excitons are provided by (6,5) carbon nanotubes that feature a substantial 400 meV exciton binding energy.[25−27] This work focuses on the ultrafast optical switching dynamics associated with the 1s-exciton resonance of the lowest subband. As shown in Figure 1b, our nanotubes are randomly oriented within an aqueous dispersion, which

Received: February 26, 2020
Published: May 6, 2020

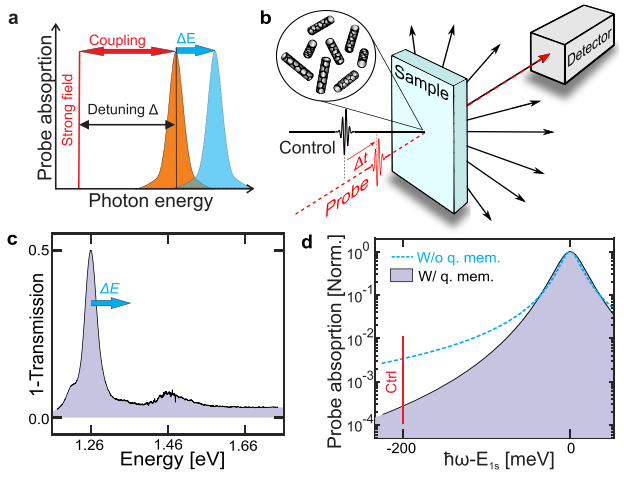

Figure 1. Concept of ultrafast optical switching with carbon nanotubes. (a) A 1s-exciton resonance (orange peak) becomes shifted (blue peak) by ΔE when a strong optical field is detuned well below the 1s-exciton state. (b) An aqueous suspension of high-purity (6,5)-enriched carbon nanotubes is probed normally and controlled with a separate angle with respect to the probe, as a function of control–probe delay Δt. (c) Measured linear probe transmission without control pulse. (d) Computed probe absorption with (shaded area, using eq 3) and without (dashed line, using eq 2) quantum memory. The red vertical line indicates the central photon energy of the control pulse.

ensures that control-generated coherences couple to any, including the probe direction, to create the ΔE shift. Figure 1c presents the measured probe transmission spectrum of this sample. The spectrum consists of the 1s-exciton peak at 1.26 eV as well as the corresponding phonon sideband peak at 1.46 eV, respectively. Also, smaller peaks appear at 1.23 and 1.35 eV due to exciton resonances of residual populations of (7,5) and (9,1) nanotubes in the sample.

In our computations, we self-consistently solve the Maxwell–semiconductor Bloch equations[29] for (6,5) nanotubes, and microscopically include dephasing kinetics to describe the possible irreversibility in the proposed optical switch. In our setup, the control field is a strong control pulse that creates both polarization P_k and electron–hole distributions $f_k^{e(h)}$ at the carrier momentum $\hbar k$. Once created, P_k experiences excitation-induced dephasing that is dominated by Coulombic scattering, even at room temperature. This will induce both excitation-induced broadening for the exciton resonance and eventually irreversibility for the switching.

In a phenomenological description, the decoherence dynamics of the polarization can be parametrized by an instantaneous decay

$$\left.\frac{\partial}{\partial t}P_k(t)\right|_{\text{instant}} = -\gamma P_k(t) \tag{2}$$

quantified by a single dephasing constant γ. Microscopically, γ results from a quantum-kinetic scattering[22,29] where polarization exchanges momentum with electrons and holes, and this process always takes some time to build up. Following the key observations of ref 28, we show in the Supporting Information that the fully kinetic, microscopic scattering actually introduces quantum memory:

$$\left.\frac{\partial}{\partial t}P_k(t)\right|_{\text{Q-memory}} = -\frac{\gamma}{T_{\text{QM}}}\int_{-\infty}^{t} \mathrm{d}t'[e^{-i/\hbar\hat{H}_{\text{ex}}(t-t')}P(t')]_k e^{-(t-t')/T_{\text{QM}}} \tag{3}$$

where $e^{-i/\hbar\hat{H}_{\text{ex}}t}$ propagates the excitonic polarization and T_{QM} defines how fast dephasing is built up due to quantum memory. Consequently, the decay of polarization at time t depends on the polarization at earlier times $t' < t$, introducing quantum memory to scattering as is common for excitation-induced dephasing.[28] Unlike for resonant excitations, detuned $P(t')$ and $e^{i/\hbar\hat{H}_{\text{ex}}t'}$ contributions remain out of phase during the past time t' so that adding up all past polarizations partially average out in the memory integral (eq 3), making effective dephasing much weaker for detuned than it is for resonant excitations. In our system, the quantum memory kernel is found to last for T_{QM} = 66 fs, which is long enough to reduce the irreversibility of nonresonant excitations. Figure 1d shows that computations with (shaded area, using eq 3) and without (dashed line, with eq 2) quantum memory produce essentially identical absorption values close to the 1s resonance. For energies well below the 1s-exciton state, the instantaneous dephasing produces a far-reaching Lorentzian tail suppressed by 1 order of magnitude at Δ = −200 meV by the quantum memory. The proposed switch concept harnesses quantum memory to eliminate dephasing, that is, irreversibility from the transient Stark shift, by using a sufficiently large detuning for the control pulse.

Our 200 fs control pulse is detuned Δ = −200 meV below the 1s-exciton resonance. Figure 2a compares the measured probe transmission without (shaded areas) and with (red lines) the control pulse for three representative control–probe

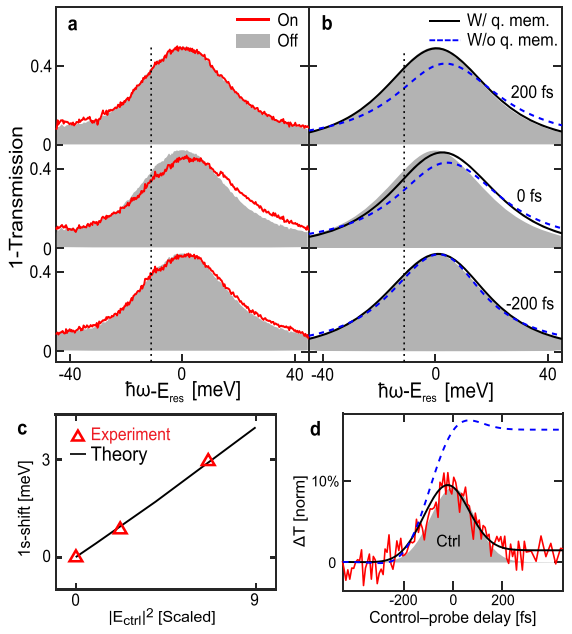

Figure 2. Experiment–theory demonstration of ultrafast optical switching. (a) Measured vs (b) computed probe transmission spectra without (shaded area) and with (solid lines) control pulse for three representative control–probe time delays. The dashed line shows the results computed without quantum memory, using a phenomenological decay constant (2) instead of its full quantum-kinetic form (3). (c) Computed (solid line) vs measured Stark shift (triangles) ΔE at 0 time delay as a function of control pulse intensity $|E_{\text{ctrl}}|^2$. (d) Time-resolved switching of probe transmission 10 meV below the 1s-exciton state. Measured (red line) change is compared to computations with (black line) and without (dashed line) quantum memory. The shaded area indicates the envelope of the control pulse.

https://dx.doi.org/10.1021/acsphotonics.0c00315
ACS Photonics 2020, 7, 1382−1387

time delays (peak-to-peak), while the probe spectrum at −200 fs matches the no control-pulse base (full data is presented in the Supporting Information). It becomes visibly blue-shifted during the control pulse, roughly by ΔE = 3 meV for 0 fs. At the same time, the peak intensity decreases and the spectrum broadens. At 200 fs, this 1s-exciton peak returns to its original position and line shape very rapidly. The computations with (solid lines) and without (dashed lines) quantum memory are shown in Figure 2b. Only the quantum-memory computations reproduce the experimental observations quantitatively. In sharp contrast to this, the instantaneous dephasing (without quantum memory) predicts an excessive excitation-induced blue shift that is both too large and incorrectly irreversible after the control pulse. Therefore, the measured reversible transmission changes originate from the quantum-memory effects that eliminate irreversible absorption that would leave the system excessively excited after the control pulse.

Figure 2c shows that the experiments (triangles) and computations (line) produce the same shift ΔE (determined at 0 fs), and the same linear scaling in $|E_{ctrl}|^2$, which verifies the expected Stark-shift dependency of eq 1. Our highest experimental peak-field strength in Figure 2c is 1.0 MV/cm = 100 mV/nm, which is close to the threshold of generating multiphoton transitions[30] that tend to saturate the 1s shift, which we confirm to appear for field strengths exceeding roughly 130 mV/nm. This is not unexpected because such fields change potential energy by more than 100 mV across the exciton radius, inducing strong nonlinearities. We also follow the change ΔT in probe transmission as the explicit optical switch signal at a fixed frequency, here 10 meV below the 1s-exciton resonance. The dynamics of the measured (red line) and computed (solid line) ΔT are shown in Figure 2d; the dashed line corresponds to the computation without quantum memory. The optically switched ΔT follows the temporal envelope of the control pulse (shaded area) adiabatically such that switching happens here in roughly 200 fs, matching the duration of the control pulse. Analogous adiabatic transition has been detected[31] in carbon nanotubes using roughly 600 meV detuning. We observe that both experiment and computations do introduce a slight irreversibility, about 10% with respect to the peak signal, whereas computations with instantaneous decay imply a complete saturation of the signal due to excessive residual excitations. Figure 1d confirms that the quantum memory (black line) reduces the residual excitation and guarantees the adiabatic following of the electron−hole excitations with respect to transient, nonresonant control pulse needed for nearly ideal switching properties.

While the quantum memory makes optical switching functionally possible in the detuned excitation case, it is not expected to change resonant excitations based on Figure 1d. Nevertheless, this regime may produce other optical nonlinearities, such as resonant Rabi splitting and wave-mixing features, due to a spectrally degenerate control and probe. After careful experiment−theory calibrations, presented in the Supporting Information, we detune the control pulse to be resonant Δ = 0 meV and reduce the field strength by a factor of 4.87. By only changing the excitation conditions but none of the many-body details in the computations, our experiment−theory comparisons rigorously connect the many-body aspects of the resonant and nonresonant cases (Figure 2) and assign the key differences between them. Figure 3 compares measured and computed transmission spectra in the resonant

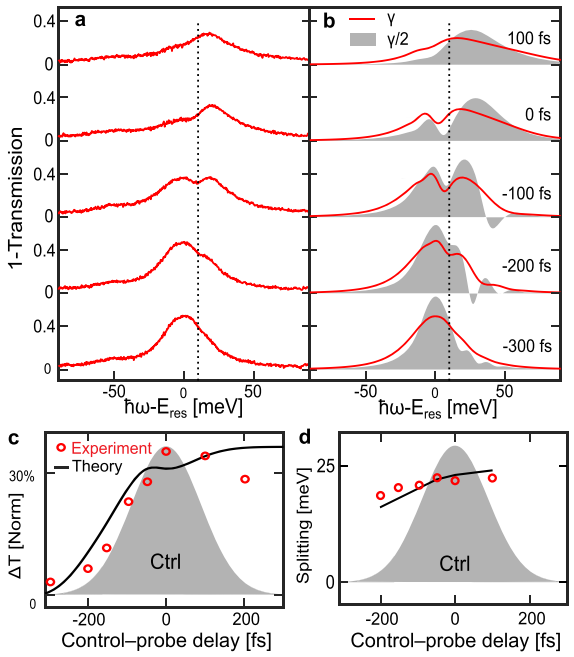

Figure 3. Irreversible switching characteristics of resonant excitations. (a) Measured vs (b) computed probe transmission spectra with actual (red lines) and artificially reduced dephasing (shaded areas) for five representative control−probe time delays. (c) Time-resolved probe transmission detuned 10 meV above the 1s state. (d) Corresponding spectral peak-splitting for computations (solid line) and experiments (open circles).

excitation case, Δ = 0. During the control pulse, from −200 to 100 fs, the 1s-exciton peak redshifts and splits into two well-separated peaks. In addition, the peak intensity decreases and broadens within the control−probe overlap duration. The spectra exhibit a distinct double-peak structure already before the control pulse, and change irreversibly after the pulse, as quantified further in Figure 3c (see also full spectral data in Supporting Information). This verifies the prediction of eq 3 that dephasing and irreversibility becomes significant for resonant excitations.

The spectral splitting in Figure 3d does not appear to follow the control-field $|E_{ctrl}(t)|$ (shaded area) as it should for Rabi splitting, based on eq 1, with Δ = 0. To uncover possible coherent effects through computations, we reduce the dephasing in eq 3 by a factor of 2, which reveals multiple peaks in the spectra (Figure 3b, shaded areas) for negative delays, when the probe arrives before the control pulse. These are the well-known coherent oscillations[32] that appear in the coherently coupled control and probe whenever the control pulse arrives after the probe and, hence, abruptly quenches the probe coherences, which is observed as spectral ringing. In our particular case, spectral splitting is related to such wave-mixing features that remain visible even at positive delays.

To improve the switching further, we only need to explore the case with large negative detuning because only it yields better reversibility for the current system. In our experiment, the exciton line width is about 20 meV before excitations, which is the expected scale at room temperature (k_BT = 26 meV at T = 300 K). With further optimized sample growth conditions and a lower temperature of measurements, reducing the exciton line width by half should be realizable.[33] Additionally, a larger Δ can reduce the generated electron−

https://dx.doi.org/10.1021/acsphotonics.0c00315
ACS Photonics 2020, 7, 1382−1387

hole density and the irreversibility due to excitation-induced effects. To keep the Stark shift constant, we increase also the control field strength together with Δ, based on eq 1. We explore improving switching performance by using an improved sample with halved background dephasing, as well as doubled $|E_{ctrl}|^2$ and detuning. As a stress test, we switch the probe transmission with eight consecutive nonresonant control pulses separated by 1 ps, each identical as that used in Figure 2. Figure 4a presents the computed transmission change observed

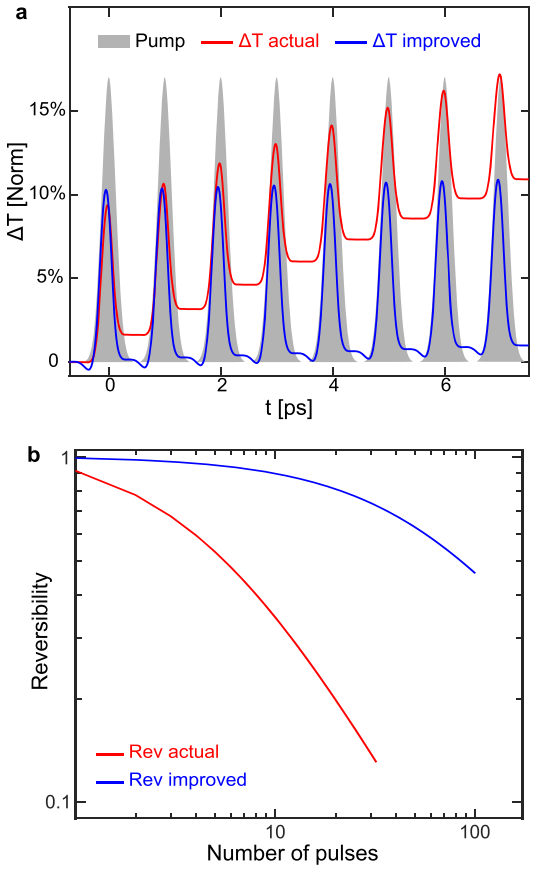

Figure 4. Limits of ultrafast optical switching. (a) Computed change in probe-transmission ΔT is followed during eight 200 fs control pulses for parameters matching the experiment (red line) and using an improved sample parameters (blue line). (b) The level of reversibility after the last pulse, as a function of pulse number for experimental (red line) and 50%-reduced dephasing (blue line) conditions.

by the probe using parameters matching the actual (red line) and the improved (blue line) sample. We see a sizable switching signal and reversibility after each pulse in both cases. Although the accumulated residually generated electrons and holes eventually deteriorate the reversibility, it is significantly less for the ideal sample.

To quantify how many times the optical switch can be operated, we define reversibility

$$\mathrm{Rev} = \frac{\Delta T_{peak} - \Delta T_{base}}{\Delta T_{peak}} \tag{4}$$

as the ratio of the peak transmission change ΔT_{peak} compared to the base transmission ΔT_{base} that is the average value of transmission before and after switching. Reversibility close to unity signifies robust reversibility, while values close to zero imply complete saturation of the switch. Figure 4b presents reversibility for the actual (red line) and the improved (blue line) sample as a function of the number of switching pulses used. We conclude that the reversibility of the improved sample decays 20× slower than that of the actual sample, yielding a reversibility as high as 10% after more than 500 pulses.

In conclusion, we have demonstrated that carbon nanotubes can be used for ultrafast optical switching that is nearly reversible when control pulses are clearly nonresonant. Our system exhibits reversibility up to tens of control pulses with 1 ps or possibly shorter temporal separation, and can be significantly improved to hundreds by optimizing the excitonic line widths. This capability can open the path to coherently switch optoelectronics at least terahertz clock rates matching the 1 ps pulse separations tested here.

METHODS

Experiments. The sample consists of (6,5)-enriched carbon nanotubes dispersed in a solution contained within a quartz cuvette with an optical path length of 1 mm. The chirality purity is as high as 93%. This is obtained by taking a high-pressure carbon monoxide (HiPco)-grown mixture containing many different chiralities of carbon nanotubes and performing a gel-chromatography technique on this mixture to isolate a solution containing (6,5)-enriched carbon nanotubes, as described in ref 34. Optical switching is measured using the Ti:sapphire-based chirped pulse amplifier (Clark-MXR, Inc., CPA 2010), which delivers output pulses of 775 nm (1.6 eV) at 1 kHz with an average power up to 1.2 W and a pulse duration of 200 fs. The laser output is split into two beams. One beam containing 90% of its output power is used to pump the optical parametric amplifier (OPA), capable of delivering intense tunable control pulses with a photon energy ranging from 0.07 to 2.34 eV. The other beam containing the remaining 10% of the CPA output is focused onto a sapphire crystal to generate a white-light continuum used as the optical probe. The ultrafast control−probe measurements are performed in a transmission geometry. Only the transmitted white-light continuum probe beam is collected and sent to a spectrometer equipped with a charge-coupled device (CCD) camera. The delay time between the control pulse and the probe pulse is controlled by a mechanical stage. The differential transmission at a certain time delay $T(t)$ is calculated via

$$T(t) = \frac{I(t) - I_0(t)}{I_0(t)} \tag{5}$$

where I and I_0 are the transmitted white-light intensity with and without the control pulse, respectively. More experimental details as well as diagrams are presented in the Supporting Information.

Theory. The studied system consists of (6,5) carbon nanotubes that are direct-gap semiconductors with a 1.26 eV gap energy, while the next confinement level has a 2.17 eV gap.[34,35] We study here ultrafast switching close to the 1.26 eV gap so that electronic excitations involve essentially only two bands. The optical nonlinearities of the carbon nanotube response are systematically solved with the semiconductor Bloch equations (SBEs)[29,36]

https://dx.doi.org/10.1021/acsphotonics.0c00315
ACS Photonics 2020, 7, 1382−1387

$$i\hbar\frac{\partial}{\partial t}P_k = \tilde{E}_k P_k - (1 - f_k^{e} - f_k^{h})\Omega_k + \Gamma_k$$

$$\hbar\frac{\partial}{\partial t}f_k^{e(h)} = 2\mathrm{Im}[P_k\Omega_k^{*}] + \Gamma_k^{e(h)} \quad (6)$$

where P_k is the microscopic polarization at momentum $\hbar k$, $f_k^{e(h)}$ is the microscopic electron (hole) occupation, $\tilde{E}_k = E_k - \sum_{k'} V_{k-k'}(f_{k'}^{e} + f_{k'}^{h})$ is the renormalized electron−hole energy with bandgap energy E_k and Coulomb matrix element V_k, and $\Omega_k = d_k \cos\theta E(t) + \sum_{k'} V_{k-k'}P_{k'}$ is the renormalized Rabi energy, with a dipole matrix element d_k, an optical field E, and the angle θ between them. We systematically couple SBEs to Maxwell's equations to compute a self-consistent transmission[28,29] measured in experiments. Band structure as well as Coulomb- and dipole-matrix elements of the carbon nanotube are determined using a tight-binding model, outlined in ref 24. The two-body correlations Γ_k^{λ} introduce Coulomb and phonon-introduced scattering. On the ultrafast time scale, Γ_k is dominated by Coulombic dephasing and described by the quantum-memory integral in eq 3. The detailed derivation of quantum memory is presented in the Supporting Information. There, the exciton propagator is found to involve an effective Hamiltonian

$$[\hat{H}_{ex}]_{k,K} = \delta_{k,K}\tilde{E}_k - (1 - f_k^{e} - f_k^{h})V_{k-K} \quad (7)$$

This uniquely defines excitons via an eigenvalue problem in the form of the generalized Wannier equation[29]

$$[\hat{H}_{ex}\phi_\lambda]_k = \sum_K [\hat{H}_{ex}]_{k,K}\phi_\lambda(K) = E_\lambda\phi_\lambda(k) \quad (8)$$

where $\phi_\lambda(k)$ is the exciton wave function and E_λ is the corresponding exciton energy.

Besides quantum memory, Coulombic scattering introduces density dependence to the γ. These experiments are quantitatively explained by using $\gamma = \gamma(n_{eh}) = 12.5\ \mathrm{meV}\left(1 + \frac{n_{eh}}{n_0}\right)$ as a function of electron (hole) density n_{eh}, normalized by $n_0 = 5.63 \times 10^4\ \mathrm{cm}^{-1}$. The macroscopic polarization $P_k = \frac{1}{L}\sum_k d_k P_k$ defines the optical transmission. Technically, we solve $P_{k,\theta}$ from SBEs for each randomly oriented nanotube labeled by angle θ with respect to probe direction. The total macroscopic polarization then becomes $P = \int_0^{\pi/2} \mathrm{d}\theta \sin\theta \cos\theta \sum_k \mathrm{d}_k P_{k,\theta}$.

■ ASSOCIATED CONTENT

Supporting Information

The Supporting Information is available free of charge at https://pubs.acs.org/doi/10.1021/acsphotonics.0c00315.

Experimental setup and calibration; Microscopic theory of quantum-memory contributions; Quantifying resonant vs nonresonant excitation conditions; Full spectra for nonresonant and resonant excitation (PDF)

■ AUTHOR INFORMATION

Corresponding Author

Mackillo Kira − *Department of Electrical and Computer Engineering and Department of Physics, University of Michigan, Ann Arbor, Michigan 48109, United States*; Email: mackkira@umich.edu

Authors

Kankan Cong − *Department of Electrical and Computer Engineering, Rice University, Houston, Texas 77005, United States*

Weiwei Jiang − *Department of Electrical and Computer Engineering, University of Michigan, Ann Arbor, Michigan 48109, United States*; orcid.org/0000-0002-7709-9825

Bryan E. Anthonio − *Department of Electrical and Computer Engineering, Rice University, Houston, Texas 77005, United States*

G. Timothy Noe − *Department of Electrical and Computer Engineering, Rice University, Houston, Texas 77005, United States*

Huaping Liu − *Beijing National Laboratory for Condensed Matter Physics, Institute of Physics, Chinese Academy of Sciences, Beijing 100190, China*; orcid.org/0000-0001-7017-4127

Hiromichi Kataura − *Nanomaterials Research Institute, National Institute of Advanced Industrial Science and Technology, Tsukuba, Ibaraki 305-8565, Japan*; orcid.org/0000-0002-4777-0622

Junichiro Kono − *Department of Electrical and Computer Engineering, Department of Physics and Astronomy, and Department of Materials Science and NanoEngineering, Rice University, Houston, Texas 77005, United States*; orcid.org/0000-0002-4195-0577

Complete contact information is available at: https://pubs.acs.org/10.1021/acsphotonics.0c00315

Author Contributions

‡These authors contributed equally to this work (K.C. and W.J.). K.C., W.J., M.K., and J.K. conceived the switching concept, K.C., B.E.A., G.T.N., and J.K. carried out the experiment and analyzed the data, H.L. and H.K. provided, processed, and characterized the sample. W.J. and M.K. developed the many-body theory and computations, as well as analyzed the data. All authors discussed the results and contributed to the writing of the manuscript.

Notes

The authors declare no competing financial interest.

■ ACKNOWLEDGMENTS

This work was supported by the University of Michigan College of Engineering Blue Sky Research Program, the Basic Energy Science (BES) program of the U.S. Department of Energy through Grant No. DE-FG02-06ER46308 (for optical experiments), the U.S. National Science Foundation through Grant No. ECCS-1708315 (for sample preparation), the Robert A. Welch Foundation through Grant No. C-1509 (for sample characterization), and the National Natural Science Foundation of China (Grant Nos. 51820105002 and 11634014).

■ REFERENCES

(1) Nakamura, S.; Ueno, Y.; Tajima, K. Femtosecond switching with semiconductor-optical-amplifier-based symmetric Mach−Zehnder-type all-optical switch. *Appl. Phys. Lett.* **2001**, *78*, 3929−3931.

(2) Johnston, W.; Prineas, J.; Smirl, A. L. Ultrafast all-optical polarization switching in Bragg-spaced quantum wells at 80 K. *J. Appl. Phys.* **2007**, *101*, 046101.

(3) Dimitriadou, E.; Zoiros, K. On the design of ultrafast all-optical NOT gate using quantum-dot semiconductor optical amplifier-based

Mach−Zehnder interferometer. *Opt. Laser Technol.* **2012**, *44*, 600−607.
(4) Nozaki, K.; Tanabe, T.; Shinya, A.; Matsuo, S.; Sato, T.; Taniyama, H.; Notomi, M. Sub-femtojoule all-optical switching using a photonic-crystal nanocavity. *Nat. Photonics* **2010**, *4*, 477.
(5) Glesk, I.; Bock, P. J.; Cheben, P.; Schmid, J. H.; Lapointe, J.; Janz, S. All-optical switching using nonlinear subwavelength Mach−Zehnder on silicon. *Opt. Express* **2011**, *19*, 14031−14039.
(6) Volz, T.; Reinhard, A.; Winger, M.; Badolato, A.; Hennessy, K. J.; Hu, E. L.; Imamoğlu, A. Ultrafast all-optical switching by single photons. *Nat. Photonics* **2012**, *6*, 605.
(7) Press, D.; De Greve, K.; McMahon, P. L.; Ladd, T. D.; Friess, B.; Schneider, C.; Kamp, M.; Höfling, S.; Forchel, A.; Yamamoto, Y. Ultrafast optical spin echo in a single quantum dot. *Nat. Photonics* **2010**, *4*, 367.
(8) Kim, D.; Carter, S. G.; Greilich, A.; Bracker, A. S.; Gammon, D. Ultrafast optical control of entanglement between two quantum-dot spins. *Nat. Phys.* **2011**, *7*, 223.
(9) Autler, S. H.; Townes, C. H. Stark effect in rapidly varying fields. *Phys. Rev.* **1955**, *100*, 703.
(10) Wagner, M.; Schneider, H.; Stehr, D.; Winnerl, S.; Andrews, A. M.; Schartner, S.; Strasser, G.; Helm, M. Observation of the Intraexciton Autler-Townes Effect in GaAs/AlGaAs Semiconductor Quantum Wells. *Phys. Rev. Lett.* **2010**, *105*, 167401.
(11) Mollow, B. R. Power Spectrum of Light Scattered by Two-Level Systems. *Phys. Rev.* **1969**, *188*, 1969−1975.
(12) Roy, C.; Hughes, S. Phonon-dressed Mollow triplet in the regime of cavity quantum electrodynamics: excitation-induced dephasing and nonperturbative cavity feeding effects. *Phys. Rev. Lett.* **2011**, *106*, 247403.
(13) Yoshie, T.; Scherer, A.; Hendrickson, J.; Khitrova, G.; Gibbs, H.; Rupper, G.; Ell, C.; Shchekin, O.; Deppe, D. Vacuum Rabi splitting with a single quantum dot in a photonic crystal nanocavity. *Nature* **2004**, *432*, 200.
(14) Brune, M.; Schmidt-Kaler, F.; Maali, A.; Dreyer, J.; Hagley, E.; Raimond, J.; Haroche, S. Quantum Rabi oscillation: A direct test of field quantization in a cavity. *Phys. Rev. Lett.* **1996**, *76*, 1800.
(15) Reithmaier, J. P.; Sęk, G.; Löffler, A.; Hofmann, C.; Kuhn, S.; Reitzenstein, S.; Keldysh, L.; Kulakovskii, V.; Reinecke, T.; Forchel, A. Strong coupling in a single quantum dot−semiconductor microcavity system. *Nature* **2004**, *432*, 197.
(16) Khitrova, G.; Gibbs, H.; Kira, M.; Koch, S. W.; Scherer, A. Vacuum Rabi splitting in semiconductors. *Nat. Phys.* **2006**, *2*, 81.
(17) Forn-Díaz, P.; Lamata, L.; Rico, E.; Kono, J.; Solano, E. Ultrastrong coupling regimes of light-matter interaction. *Rev. Mod. Phys.* **2019**, *91*, 025005.
(18) Frisk Kockum, A.; Miranowicz, A.; De Liberato, S.; Savasta, S.; Nori, F. Ultrastrong coupling between light and matter. *Nat. Rev. Phys.* **2019**, *1*, 19−40.
(19) Haug, H.; Koch, S. W. *Quantum Theory of the Optical and Electronic Properties of Semiconductors*, 5th ed.; World Scientific Publishing Company: Hackensack, 2009.
(20) Wang, H.; Ferrio, K.; Steel, D. G.; Hu, Y.; Binder, R.; Koch, S. W. Transient nonlinear optical response from excitation induced dephasing in GaAs. *Phys. Rev. Lett.* **1993**, *71*, 1261.
(21) Shacklette, J. M.; Cundiff, S. T. Role of excitation-induced shift in the coherent optical response of semiconductors. *Phys. Rev. B: Condens. Matter Mater. Phys.* **2002**, *66*, 045309.
(22) Smith, R.; Wahlstrand, J.; Funk, A.; Mirin, R.; Cundiff, S.; Steiner, J.; Schafer, M.; Kira, M.; Koch, S. W. Extraction of many-body configurations from nonlinear absorption in semiconductor quantum wells. *Phys. Rev. Lett.* **2010**, *104*, 247401.
(23) Monniello, L.; Tonin, C.; Hostein, R.; Lemaitre, A.; Martinez, A.; Voliotis, V.; Grousson, R. Excitation-induced dephasing in a resonantly driven InAs/GaAs quantum dot. *Phys. Rev. Lett.* **2013**, *111*, 026403.
(24) Malic, E.; Knorr, A. *Graphene and Carbon Nanotubes: Ultrafast Optics and Relaxation Dynamics*; John Wiley & Sons: Weinheim, 2013.
(25) Maultzsch, J.; Pomraenke, R.; Reich, S.; Chang, E.; Prezzi, D.; Ruini, A.; Molinari, E.; Strano, M.; Thomsen, C.; Lienau, C. Exciton binding energies in carbon nanotubes from two-photon photoluminescence. *Phys. Rev. B: Condens. Matter Mater. Phys.* **2005**, *72*, 241402.
(26) Dukovic, G.; Wang, F.; Song, D.; Sfeir, M. Y.; Heinz, T. F.; Brus, L. E. Structural dependence of excitonic optical transitions and band-gap energies in carbon nanotubes. *Nano Lett.* **2005**, *5*, 2314−2318.
(27) Wang, F.; Dukovic, G.; Brus, L. E.; Heinz, T. F. The optical resonances in carbon nanotubes arise from excitons. *Science* **2005**, *308*, 838−841.
(28) Kira, M.; Koch, S. W. Many-body correlations and excitonic effects in semiconductor spectroscopy. *Prog. Quantum Electron.* **2006**, *30*, 155−296.
(29) Kira, M.; Koch, S. W. *Semiconductor Quantum Optics*; Cambridge University Press: New York, 2012.
(30) Akimov, D. A.; Alfimov, M. V.; Konorov, S. O.; Ivanov, A. A.; Botti, S.; Podshivalov, A. A.; Ciardi, R.; Dominicis, L. D.; Asilyan, L. S.; Fantoni, R.; Zheltikov, A. M. Second- and third-harmonic generation by carbon nanotubes irradiated with femtosecond laser pulses. *J. Exp. Theor. Phys.* **2004**, *98*, 220−226.
(31) Song, D.; Wang, F.; Dukovic, G.; Zheng, M.; Semke, E. D.; Brus, L. E.; Heinz, T. F. Measurement of the optical Stark effect in semiconducting carbon nanotubes. *Appl. Phys. A: Mater. Sci. Process.* **2009**, *96*, 283−287.
(32) Joffre, M.; la Guillaume, C. B. a; Peyghambarian, N.; Lindberg, M.; Hulin, D.; Migus, A.; Koch, S. W.; Antonetti, A. Coherent effects in pump−probe spectroscopy of excitons. *Opt. Lett.* **1988**, *13*, 276−278.
(33) Srivastava, A.; Htoon, H.; Klimov, V. I.; Kono, J. Direct Observation of Dark Excitons in Individual Carbon Nanotubes: Inhomogeneity in the Exchange Splitting. *Phys. Rev. Lett.* **2008**, *101*, 087402.
(34) Liu, H.; Nishide, D.; Tanaka, T.; Kataura, H. Large-scale single-chirality separation of single-wall carbon nanotubes by simple gel chromatography. *Nat. Commun.* **2011**, *2*, 309.
(35) Lim, Y.-S.; et al. Ultrafast generation of fundamental and multiple-order phonon excitations in highly enriched (6, 5) single-wall carbon nanotubes. *Nano Lett.* **2014**, *14*, 1426−1432.
(36) Hirtschulz, M.; Milde, F.; Malić, E.; Butscher, S.; Thomsen, C.; Reich, S.; Knorr, A. Carbon nanotube Bloch equations: A many-body approach to nonlinear and ultrafast optical properties. *Phys. Rev. B: Condens. Matter Mater. Phys.* **2008**, *77*, 035403.

https://dx.doi.org/10.1021/acsphotonics.0c00315
ACS Photonics 2020, 7, 1382−1387